Inorganic Chemistry

Article

pubs.acs.org/IC

A Series of Uranium (IV, V, VI) Tritylimido Complexes, Their Molecular and Electronic Structures and Reactivity with CO_2

Anna-Corina Schmidt,[†] Frank W. Heinemann,[†] Laurent Maron,[‡] and Karsten Meyer*[,†]

[†]Department of Chemistry and Pharmacy, Inorganic Chemistry, Friedrich-Alexander University of Erlangen-Nürnberg (FAU), Egerlandstr. 1, 91058 Erlangen, Germany

[‡]LPCNO, Université de Toulouse, INSA Toulouse, 135 Avenue de Rangueil, 31077 Toulouse, France

Supporting Information

ABSTRACT: A series of uranium tritylimido complexes with structural continuity across complexes in different oxidation states, namely U^{IV}, U^{V}, and U^{VI}, is reported. This series was successfully synthesized by employing the trivalent uranium precursor, $[(({}^{nP,Me}ArO)_3tacn)U^{III}]$ (**1**) (where $({}^{nP,Me}ArO)_3tacn^{3-}$ = trianion of 1,4,7-tris(2-hydroxy-5-methyl-3-neopentylbenzyl)-1,4,7-triazacyclononane), with the organic azides Me_3SiN_3, Me_3SnN_3, and Ph_3CN_3 (tritylazide). While the reaction with Me_3SiN_3 yields an inseparable mixture of both the azido and imido uranium complexes, applying the heavier Sn homologue yields the bis-μ-azido complex $[\{(({}^{nP,Me}ArO)_3tacn)U^{IV}\}_2(\mu\text{-}N_3)_2]$ (**2**) exclusively. In contrast to this one-electron redox chemistry, the reaction of precursor **1** with tritylazide solely leads to the two-electron oxidized U^{V} imido $[(({}^{nP,Me}ArO)_3tacn)U^{V}(N\text{-}CPh_3)]$ (**3**). Oxidation and reduction of **3** yield the corresponding U^{VI} and U^{IV} complexes $[(({}^{nP,Me}ArO)_3tacn)U^{VI}(N\text{-}CPh_3)][B(C_6F_5)_4]$ (**4**) and $K[(({}^{nP,Me}ArO)_3tacn)U^{IV}(N\text{-}CPh_3)]$ (**5**), respectively. In addition, the U^{V} imido **3** engages in a H atom abstraction reaction with toluene to yield the closely related amido complex $[(({}^{nP,Me}ArO)_3tacn)U^{IV}(N(H)\text{-}CPh_3)]$ (**6**). Complex **6** and the three tritylimido complexes **3**, **4**, and **5**, with oxidation states ranging from +IV to +VI and homologous core structures, were investigated by X-ray diffraction analyses and magnetochemical and spectroscopic studies as well as density functional theory (DFT) computational analysis. The series of structurally very similar imido complexes provides a unique opportunity to study electronic properties and to probe the uranium imido reactivity solely as a function of electron count of the metal−imido entity. Evidence for the U−N bond covalency and f-orbital participation in complexes **3**−**6** was drawn from the in-depth and comparative DFT study. The reactivity of the imido and amido complexes with CO_2 was probed, and conclusions about the influence of the formal oxidation state are reported.

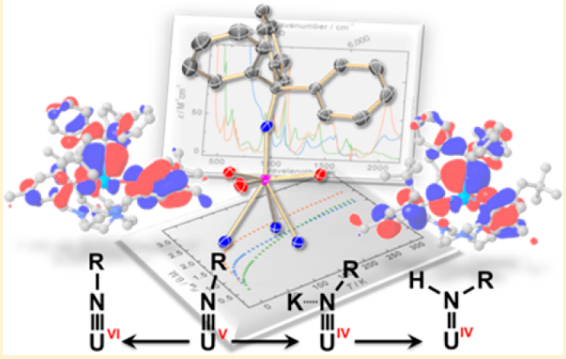

INTRODUCTION

Considering the current interest in f-element complexes with multiply bonded ligands, such as uranium imidos and nitrides, the sparse employment of Ph_3CN_3 (tritylazide) as a reagent in uranium coordination chemistry is surprising.[1] Because of its excellent leaving groups, namely N_2 and the trityl radical $Ph_3C^{\bullet}$, with subsequent formation of Gomberg's dimer, tritylazide is a valuable but underappreciated substrate for the synthesis of uranium azido and imido complexes.[2] Both of these species are potential precursors to the synthesis of uranium terminal nitrido species,[3] an exceedingly rare class of compounds limited to two reports by Liddle and co-workers.[4]

In a systematic approach, we first examined the general reactivity of the trivalent uranium precursor, $[(({}^{nP,Me}ArO)_3tacn)U^{III}]$ (**1**) (where $({}^{nP,Me}ArO)_3tacn^{3-}$ = trianion of 1,4,7-tris(2-hydroxy-5-methyl-3-neopentylbenzyl)-1,4,7-triazacyclononane), with the organic azides Me_3SiN_3, Me_3SnN_3, and Ph_3CN_3 to evaluate the systems tendency to form the one- and two-electron oxidation products, namely the azido or imido complex. Subsequently, the reactivity of the resulting imido complex was examined with special attention on redox- and CO_2-activation chemistry. In addition, the U−N bond covalency and f-orbital participation of the uranium imido and amido entity in the various oxidation states was interrogated by an in-depth and comparative density functional theory (DFT) computational analysis.

Although the synthesis of mid- to high-valent uranium azido and imido complexes from inorganic and organic azides has long been established,[5] a homologous series of structurally, spectroscopically, and theoretically studied uranium imido complexes over a range of accessible oxidation states is currently absent from the literature.

Recently, Schelter et al. reported the synthesis of the U^{V} imido complex $[((Me_3Si)_2N)_3U(N\text{-}CPh_3)]$ via the two-electron oxidation of the parent U^{III} tris(amido) complex with tritylazide.[1b] Interestingly, the same study also reports a rather unexpected one-electron oxidation of the U^{IV} azido

Received: September 26, 2014
Published: November 26, 2014

   dx.doi.org/10.1021/ic5023517 | Inorg. Chem. 2014, 53, 13142−13153

species $[((Me_3Si)_2N)_3U(N_3)]$ with tritylazide and subsequent addition of *N*-methylmorpholine-*N*-oxide to yield a structurally identical U^V imido complex. While most crystallographically characterized imido complexes reported in the literature were synthesized in only one oxidation state, the latter protocol provided access to both the reduced and oxidized imido complexes, with crystallographic characterization of the U(V) and U(IV) species.[1b] Related to this and our study is the most recent work by Boncella et al., reporting a series of [U═NDipp] (Dipp = 2,6-diisopropylphenyl)imido complexes in oxidation states IV, V, and VI, each with noticeably different molecular structures and chemical compositions, however.[5n] In the Boncella paper, substitution of two chloride ligands of $[(Me_2bpy)_2U^{IV}(Cl)_4]$ by LiNHDipp yields the terminal imido U^{IV} complex $[(Me_2bpy)_2U^{IV}(NDipp)(Cl)_2]$, which is oxidized by additional LiNHDipp to form the bis-imido U^V complex $[(Me_2bpy)_2U^V(NDipp)_2(Cl)]$. Starting from the *tert*-butyl derivative $[(^tBu_2bpy)_2U^{IV}(Cl)_4]$, reaction with excess LiNHDipp and subsequent oxidation with iodine leads to the bis-imido U^{VI} complex $[(^tBu_2bpy)U^{VI}(NDipp)_2(I)_2]$.

Very recently, Bart et al. published a unique series of uranium mono-, bis-, and tris(mesitylimido) complexes in oxidation states +IV to +VI, namely $[(^{Mes}PDI^{Me})U(NMes)(I)_2(THF)]$, $[(^{Mes}PDI^{Me})U(NMes)_2(I)(THF)]$, and $[(^{Mes}PDI^{Me})U(NMes)_3]$ ($^{Mes}PDI^{Me}$ = 2,6-(mesityl-N═CMe)$_2C_5H_3N$).[6] All complexes were fully characterized, including their solid-state molecular structures. This work certainly represents a milestone in uranium coordination chemistry. However, because of the complexes' different compositions and geometries, a systematic investigation of the nature of the multiple-bonded imido ligand as a function of oxidation state in a series of structurally similar complex geometries cannot be conducted here.[6]

Aiming toward synthesizing a similar - but structurally closely related - series of mid- to high-valent metal-imido complexes, we probed the reactivity of $[((^{nP,Me}ArO)_3tacn)U^{III}]$ (**1**,[7] Chart 1) with different organic azides, namely Me_3SiN_3, Me_3SnN_3, and Ph_3CN_3 (tritylazide), thereby testing their proclivity for one- or two-electron oxidation of the uranium(III) complex.

RESULTS AND DISCUSSION

The reaction of $[((^{nP,Me}ArO)_3tacn)U^{III}]$ (**1**) with Me_3SnN_3 did not yield the expected imido complex but allowed for the isolation and characterization of the new bis-μ-azide bridged diuranium complex $[\{((^{nP,Me}ArO)_3tacn)U^{IV}\}_2(\mu\text{-}\kappa^1\text{:}\kappa^1\text{-}N_3)_2]$ (**2**). Choosing the alternative tritylazide Ph_3CN_3 reagent, however, provides convenient access to a series of three tris(aryloxide) tacn-based tritylimido complexes, namely $[((^{nP,Me}ArO)_3tacn)U(N\text{-}CPh_3)]^{-/0/+}$, which were characterized by X-ray diffraction (XRD) analysis, hence, complementing the two recent reports by Schelter and Boncella and co-workers. The newly discovered series of complexes reported here, spanning the range of accessible oxidation states +IV, +V, and +VI, exhibits uranium imido complexes with structurally virtually unperturbed core structures and provides unique insight into the covalency and f-orbital participation of the U−N multiple bond. The synthesized amido and imido complexes additionally present an opportunity to evaluate the reactivity of the U−NR entity as a function of the electronic and structural properties of three oxidation states.

Chart 1. Numbering Scheme and Abbreviations of Uranium Complexes 2−9, Obtained from the Starting Complex $[((^{nP,Me}ArO)_3tacn)U^{III}]$ (1), where $(^{nP,Me}ArO)_3tacn^{3-}$ = trianion of 1,4,7-tris(2-hydroxy-5-methyl-3-neopentylbenzyl)-1,4,7-triazacyclononane

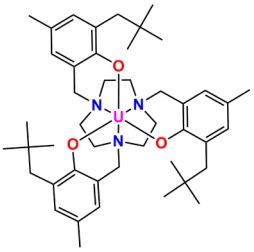

Number	Complex
1	$[((^{nP,Me}ArO)_3tacn)U^{III}]$
2	$[\{((^{nP,Me}ArO)_3tacn)U^{IV}\}_2(\mu\text{-}\kappa^1\text{:}\kappa^1\text{-}N_3)_2]$
3	$[((^{nP,Me}ArO)_3tacn)U^V(N\text{-}CPh_3)]$
4	$[((^{nP,Me}ArO)_3tacn)U^{VI}(N\text{-}CPh_3)][B(C_6F_5)_4]$
5	$K[((^{nP,Me}ArO)_3tacn)U^{IV}(N\text{-}CPh_3)]$
5a	$[K(C_6H_6)][((^{nP,Me}ArO)_3tacn)U^{IV}(N\text{-}CPh_3)]$
6	$[((^{nP,Me}ArO)_3tacn)U^{IV}(N(H)\text{-}CPh_3)]$
7	$[((^{nP,Me}ArO)_3tacn)U^{IV}(\kappa^2\text{-}O_2C\text{-}N(H)\text{-}CPh_3)]$
8	$K[((^{nP,Me}ArO)_3tacn)U^{IV}(O)]$
9	$[\{((^{nP,Me}ArO)_3tacn)U^V\}_2(\mu\text{-}O)_2]$

SYNTHESIS AND MOLECULAR STRUCTURES

Reaction of **1** with trimethylsilyl azide yields a brown solution that was examined by ^1H NMR spectroscopy and found to be an inseparable mixture of U^V imido and U^{IV} azido complexes, respectively. To direct the synthesis clearly toward the targeted imido complex, alternative azide donors were tested. The use of trimethylstannyl azide was not successful, however, and produces a new azido U^{IV} complex, namely $[\{((^{nP,Me}ArO)_3tacn)U^{IV}\}_2(\mu\text{-}\kappa^1\text{:}\kappa^1\text{-}N_3)_2]$ (**2**), exclusively. The mechanism is proposed to occur via azide ($N_3^\bullet$) and stannyl ($Me_3Sn^\bullet$) radical formation,[8] ultimately leading to the oxidation of the U^{III} to yield U^{IV}−N_3 and subsequently dimeric **2**, as well as hexamethyldistannane, Me_3Sn−$SnMe_3$, which was detected by ^1H NMR spectroscopy. Similar reactivities were reported for the reaction of U^{III} with the silyl derivative trimethylsilyl azide[5d] and for the reaction of a Zn(I) complex with the group 14 azides Me_3M−N_3 (with M = Si, Sn), yielding the corresponding oxidized metal-azido species with concomitant formation of Me_6M_2.[9]

The addition of 1 equiv of trimethylstannyl azide to **1** in tetrahydrofuran (THF) leads to an immediate color change of the reaction solution from dark-red to lime-green. After solvent evaporation and workup of the residue (see Supporting Information), lime-green **2** can be isolated in excellent yields. Bright green crystals of **2** were obtained by slow evaporation of a benzene solution of **2** and were studied by XRD. The molecular structure of **2** shows a dinuclear uranium species with the two eight-coordinated uranium ions bridged by two end-on coordinated azide ligands (Figure 1, top).

Remarkably, only a few structurally characterized uranium azido complexes have been reported; the monomeric examples

dx.doi.org/10.1021/ic5023517 | Inorg. Chem. 2014, 53, 13142−13153

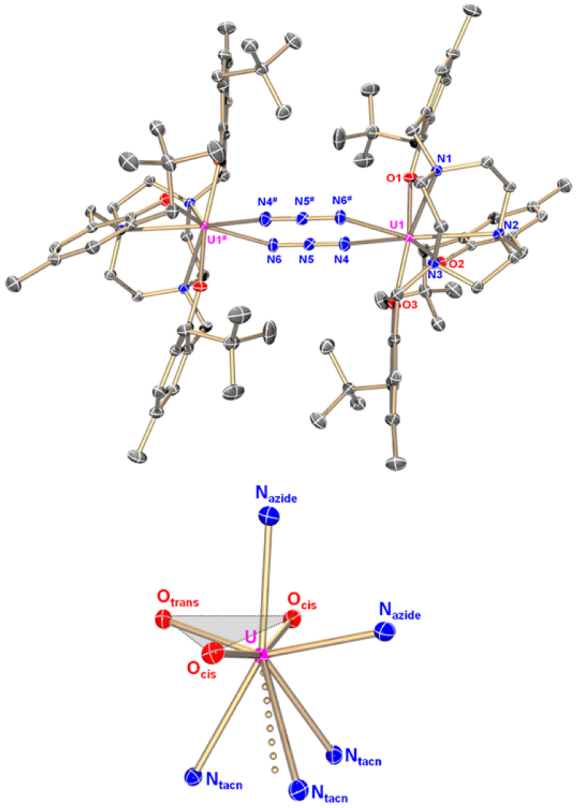

Figure 1. (top) Molecular structure of the uranium azido complex **2** in crystals of **2**·3C_6H_6. Hydrogen atoms and cocrystallized solvent molecules are omitted for clarity. Thermal ellipsoids are at 50% probability. (bottom) Core structure of complex **2** with the uranium center shown in a simplified, distorted octahedral environment. The plane defined for the U_{oop} parameter is highlighted in gray.

all exhibit azido ligands with a terminal κ^1 coordination mode.[5c,g,o,10] These examples include the rather unusual homoleptic heptaazido trianion, $[U(N_3)_7]^{3-}$.[11]

Examples of polynuclear uranium complexes with bridging azido ligands are even more exceptional[12] and include the unique octanuclear uranium ring, exhibiting alternating singly bridging nitrides (μ-N^{3-}) and azide (μ-κ^1:κ^1-N_3^-) ligands, reported by Evans et al.,[12e,13] and the tetranuclear uranium cluster reported by Mazzanti and co-workers, featuring eight bridging (μ-κ^2-N_3^-) azides.[12d] To the best of our knowledge, complexes containing more than one bridging azide with two μ-κ^1:κ^1-N_3^- ligands - as known for M = Ce or Nd in $M(\mu\text{-}N_3)_2M$ - are unprecedented in uranium coordination chemistry.[14]

In the solid-state molecular structure of **2**, the uranium ions are related to each other by a crystallographically imposed inversion center and exhibit a distorted octahedral coordination environment (vide infra). Three oxygen atoms of the aryloxide arms form a plane, and the uranium ion is shifted −0.365 Å below this plane. One end-on azide ligand is bound equatorially (eq), whereas the second azide ligand occupies the axial (ax) position opposite to the tacn anchor. The latter chelate can be considered as a single binding site, thus rendering the uranium ion coordinated in a simplified octahedral ligand environment (Figure 1, bottom). A thorough study of the electronic structure supports this geometrical simplification.[15] Although the $U-N_{ax}$ bond is slightly shorter than the $U-N_{eq}$ bond (2.509(2) and 2.558(2) Å, respectively), both bond distances are comparable to other published $U-N_{azide}$ metric parameters.[5c,12a,e] The average $U-O_{ArO}$ and $U-N_{tacn}$ bond distances of 2.180 and 2.779 Å, respectively, are in good agreement with those reported for other U^{IV} complexes of the tacn-anchored tris(aryloxide) system.[5d,e,7,16]

The U−N−N angles differ from 130.58(15)° for the axially and from 155.99(16)° for the equatorially bound azide; which is probably due to steric reasons. The metrics of the coordinated azide ligands (N_4-N_5: 1.192(2) Å, N_5-N_6: 1.163(2) Å, $\angle(N_4-N_5-N_6)$: 179.2(2)°) are almost identical to the free azide anion in 1,1-dimethylhydrazinium azide (N−N: 1.187(1) and 1.165(1) Å, $\angle(N_\alpha-N_\beta-N_\gamma)$: 178.6(1)°);[17] without any sign of coordination-induced activation of the N−N bonds of the azide. Consequentially, this reaction of complex **2** is completely reversible, as exemplified by reduction of **2** with

Scheme 1. Reaction Scheme for the Synthesis of the Imido and Amido Complexes 3−6 and the CO_2 Reaction Products 7−9[a]

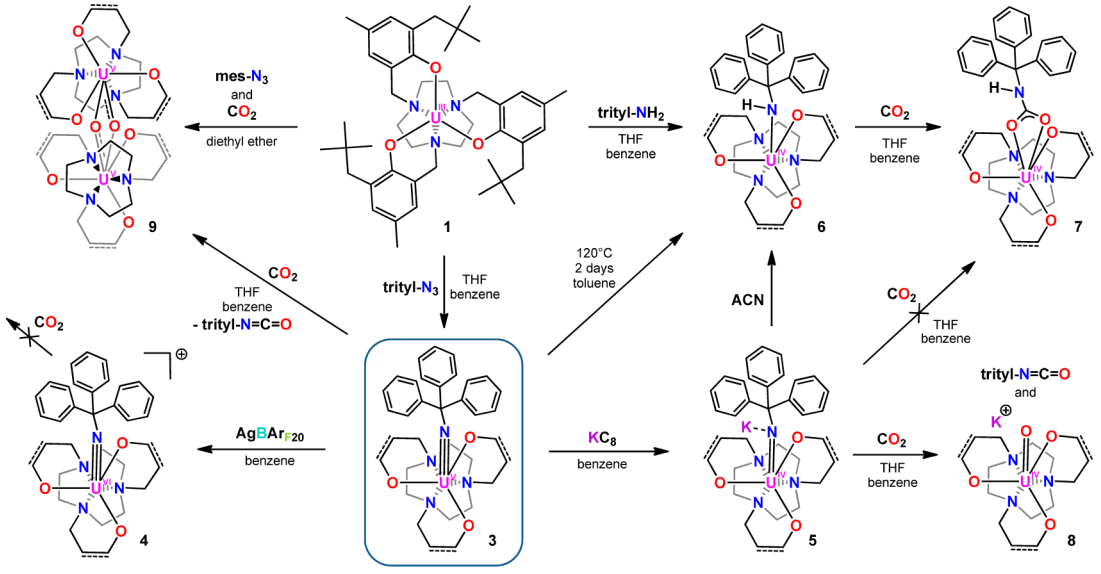

[a]Phenolate rings, including the neopentyl and methyl substituent, are omitted for clarity.

dx.doi.org/10.1021/ic5023517 | Inorg. Chem. 2014, 53, 13142−13153

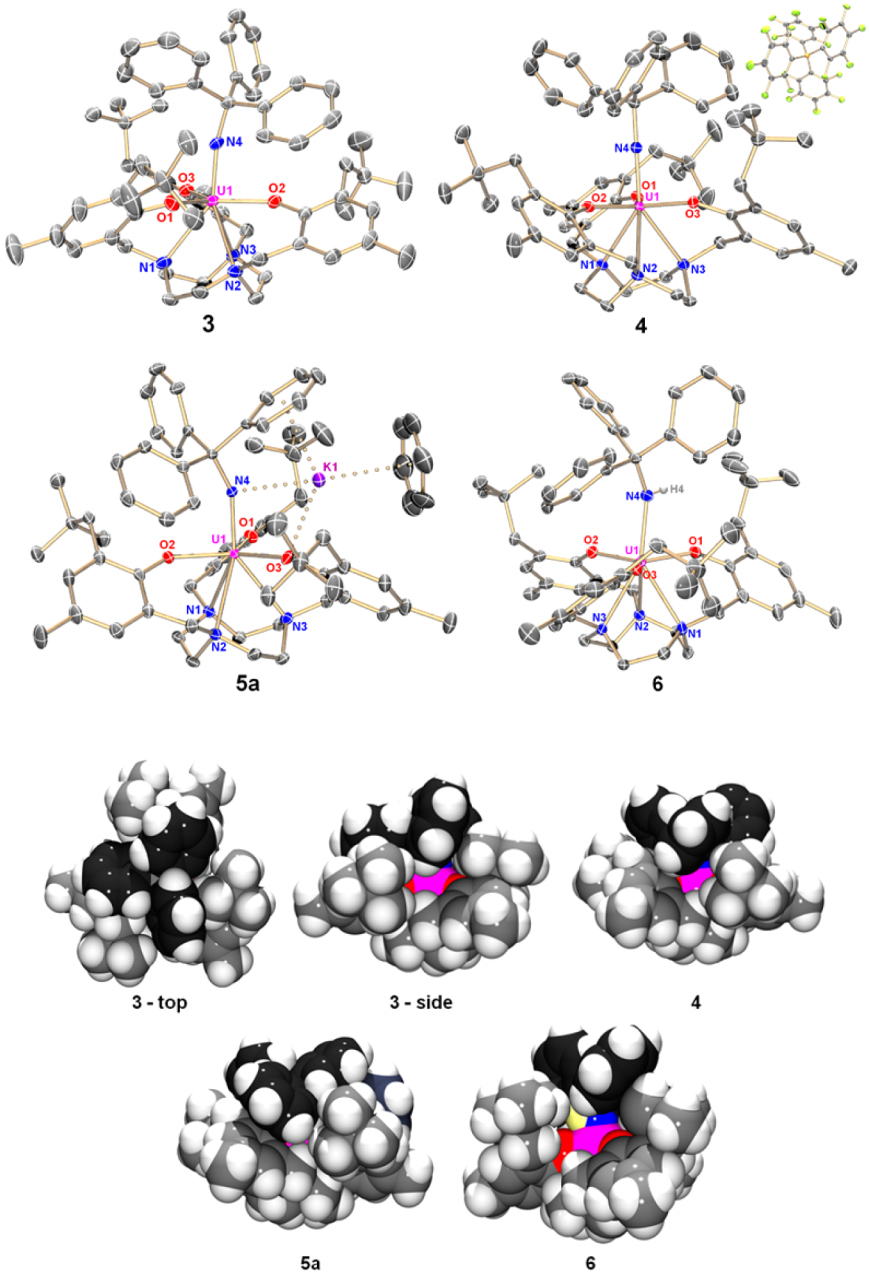

Figure 2. (top) Molecular structure of the U^{V} tritylimido complexes **3** in crystals of **3**·C_6H_6, U^{VI} (**4**) in crystals of **4**·C_6H_6, U^{IV} (**5**) in crystals of **5a**, and the U^{IV} amido complex **6** in crystals of **6**·3THF. Hydrogen atoms and cocrystallized solvent molecules are omitted for clarity. Thermal ellipsoids are at 50% probability. (bottom) Space-filling models of the uranium tritylimido complexes: top view and side view of the molecular structure of complex **3**; side view of the molecular structures of complexes **4**, **5a**, and **6**. The trityl units are highlighted in black, the additional benzene molecule in **5a** is highlighted in dark blue, and the hydrogen atom of the amido ligand in **6** is highlighted in yellow.

KC_8, yielding the U^{III} starting complex **1** and potassium azide exclusively.[18]

Given the general preference of trivalent uranium complexes to engage in one-electron redox-chemistry, the observed reactivity of **1** with Me_3SiN_3 and Me_3SnN_3 to yield the U^{IV} azido complexes was not unexpected. To this end, and considering the propensity of both reaction partners U^{III} and Ph_3CN_3 to preferentially undergo one-electron redox reaction, the envisioned synthesis of a U^{V} tritylimido complex via reaction of **1** with Ph_3CN_3 appeared to be hopeless.

Thus, it is all the more surprising that the reaction of **1** with 1 equiv of tritylazide[19] cleanly delivers the green-brown U^{V} tritylimido complex $[((^{nP,Me}ArO)_3tacn)U^{V}(N\text{-}CPh_3)]$ (**3**) in ~65% isolated yield (see Scheme 1).[20] The reaction proceeded with evolution of gaseous N_2 and without formation of any U^{IV} azido byproduct (as evidenced by ^1H NMR spectroscopy of the crude reaction product). Dark brown crystalline plates of **3**, suitable for XRD analysis, were obtained from *n*-hexane diffusion into a solution of the complex in benzene. In its molecular structure, **3** possesses a seven-coordinate uranium atom with a propeller-like, axially bound tritylimido ligand that is slightly bent and interlocking with the three neopentyl arms (Figure 2 and Table 1). Similar to transition metal-imido complexes, uranium imido species typically exhibit short, formal U≡N triple bonds, with bond lengths ranging from 1.85 to

dx.doi.org/10.1021/ic5023517 | *Inorg. Chem.* 2014, 53, 13142−13153

Table 1. Selected Bond Distances (Å) and Angles (deg) for the Imido and Amido Complexes 3−6

complex	3	4	5a	6
$U-N_{imido/amido}$	1.939(3)	1.920(2)	2.036(2)	2.253(3)
$U-O_{ArO,av}$	2.183	2.116	2.280	2.209
$U-N_{tacn,av}$	2.695	2.623	2.794	2.699
$N_{imido/amido}-C_{trityl}$	1.471(5)	1.461(3)	1.455(3)	1.467(4)
U_{oop}	−0.078	−0.142	−0.101	−0.141
$U-N_{imido/amido}-C_{trityl}$	165.0(2)	179.6(2)	153.3(2)	148.2(2)

2.12 Å and ∠(U−N−R) bond angles that vary from slightly bent to linear (154−180°).[5d,e,g,j,m,p]

Accordingly, the structural parameters of the imido complex **3**, with a $U-N_{imido}$ bond distance of 1.939(3) Å and a $U-N_{imido}-C_{trityl}$ angle of 165.0(2)°, are similar to those reported, and the U−NR moiety is best described with a U≡N triple bond (vide infra). The $N_{imido}-C_{trityl}$ bond distance is 1.471(5) Å, slightly shorter than that for the precursor tritylazide (1.517(2) Å)[19] but matching known transition metal tritylimido complexes.[21] In comparison to the only other structurally characterized U^V trityl complex, namely, $[((Me_3Si)_2N)_3U(N\text{-}CPh_3)]$,[1b] the differences of the $U-N_{trityl}$ and $N_{trityl}-C_{trityl}$ bond distances are negligible. This is despite the fact that the $U-N_{trityl}-C_{trityl}$ angle is perfectly linear in $[((Me_3Si)_2N)_3U(N\text{-}CPh_3)]$ compared to 165.0(2)° observed in **3**. This discrepancy can be attributed to the increased steric hindrance in **3**, arising from the much bulkier neopentyl-derivatized tacn-anchored tris(aryloxide) ligand system. The average $U-O_{ArO}$ and $U-N_{tacn}$ bond distances of 2.183 and 2.695 Å, respectively, are in the same range as those found in previously reported U^V imido complexes of the tris(aryloxide) tacn system.[5e] The shift of the uranium center out of the plane of the three aryloxide oxygen atoms, however, has decreased noticeably to −0.078 Å in **3** and, thus, is unusual compared to the typical values ranging from −0.151 to −0.408 Å for other tacn-based U^V imido complexes reported previously.[5c,e,15] A possible explanation is the steric repulsion of the axially bound, bulky trityl ligand and the *tert*-butyl groups of the aryloxides (Figure 2). Consequently, and because of the strong $U^{5+}-NR^{2-}$ bonding interaction, the tritylimido group draws the U ion into the plane.

Complex **3** and its ^{15}N-labeled isotopomer **3*** were investigated by IR and Raman vibrational spectroscopy (see Supporting Information, Figure S16). Isotopomer **3*** was obtained from the reaction of **1** with ^{15}N-labeled tritylazide. Despite the labeling effort, however, identification of the $U-N_{imido}$ or $N_{imido}-C_{trityl}$ bonds, expected at ∼1000 and 1280 cm^{-1}, was not possible due to the overlapping and dominating bands of the tacn chelate in the fingerprint region.[5l,22]

Uranium imido complexes with phenyl,[5a,e,h,j−m] 2,6-diisopropylphenyl,[5b,l] 2,4,6-tri-*tert*-butylphenyl,[5a,b,l] mesityl,[5e,l,m,15] adamantyl,[5k,m] and trimethylsilyl[1b,5c,j,23] substituents from reactions with the corresponding azides are quite common, but reactions leading to imido species with the sterically more encumbering triphenylmethyl (trityl) ligand are limited to a single, very recent report by Schelter and co-workers.[1b] Whereas the more commonly chosen route to tritylimido species is the alkylation of complexes with M = Cr, Fe, W, Re, and Os bearing the nitrido ligand with either the trityl radical or cation,[21a,c,24] there are few examples of tritylimido metal complexes with M = Ti, Mo, and Th obtained from reactions with the corresponding tritylazide.[2]

Unfortunately, the newly synthesized U^V imido complex **3** reacted with common electrolytes and decomposed during all attempted electrochemical investigations. Successful chemical oxidation of **3** was achieved with $AgBAr_{F20}$ (BAr_{F20}^- = tetrakis(perfluorophenyl)borate) to yield the analogous U^{VI} imido complex $[(({}^{nP,Me}ArO)_3tacn)U^{VI}(N\text{-}CPh_3)][B(C_6F_5)_4]$ (**4**), and reduction with KC_8 produced the U^{IV} imido $K[(({}^{nP,Me}ArO)_3tacn)U^{IV}(N\text{-}CPh_3)]$ (**5**). Pentavalent **3** additionally provided access to the U^{IV} amido complex $[(({}^{nP,Me}ArO)_3tacn)U^{IV}(N(H)CPh_3)]$ (**6**) when heated in toluene (see Supporting Information, Figure S6).

Oxidation of complex **3** with 1 equiv of $AgBAr_{F20}$ in benzene yields the black, diamagnetic complex $[(({}^{nP,Me}ArO)_3tacn)\text{-}U^{VI}(N\text{-}CPh_3)][B(C_6F_5)_4]$ (**4**) in moderate isolated yields (∼50%). X-ray quality crystals were obtained from slow evaporation of a benzene solution of **4**. The molecular structure of cation **4** is almost identical to that of **3** and reveals $U-N_{imido}$ and $N_{imido}-C_{trityl}$ bond distances of 1.920(2) and 1.461(3) Å, respectively. Likewise, the average $U-O_{ArO}$ and $U-N_{tacn}$ bond distances of 2.116 and 2.623 Å remain unchanged.

Minor differences can be observed for the $U-N_{imido}-C_{trityl}$ angle, which increases to 179.6(2)° (compared to 165.0(2)° in **3**), rendering the uranium imido unit almost perfectly linear. The increased linearity permits the trityl unit to reach deeper into the ligand cavity of hexavalent **4** (Figure 2), thus allowing for an increased π-overlap that results in a shorter $U-N_{imido}$ bond distance of 1.920(2) Å.[5b] Unfortunately, a high-quality crystal structure of the U^{VI} trityl complex, $[((Si\text{-}Me_3)_2N)_3U^{VI}(N\text{-}CPh_3)]^+$, for comparison with the here-reported analogous U^{VI} complex **4**, was not obtained by Schelter and co-workers.

The ^1H NMR spectrum of the C_3 symmetric, diamagnetic **4** (see Supporting Information, Figure S3) shows the expected 15 signals in a range from 7.6−1.0 ppm. Two distinct singlet signals at 7.61 and 7.52 ppm are assignable to the aryloxide hydrogen atoms. Two signals for the aromatic rings of the trityl ligand are observed at 7.22 and 6.98 ppm. The diastereotopic hydrogens of the tacn and CH_2 groups give rise to partly unresolved signals in the region from 5.2−2.2 ppm. Furthermore, one singlet at 3.49 and one at 1.00 ppm can be assigned to the methyl and *t*-butyl groups, respectively.

Addition of KC_8 to a solution of **3** in benzene leads to a gradual color change from dark red to yellow-green. After workup, the U^{IV} imido complex $K[(({}^{nP,Me}ArO)_3tacn)U^{IV}(N\text{-}CPh_3)]$ (**5**) was isolated in good yield (76%). Yellow-green crystals of the benzene-bound potassium adduct $[K(C_6H_6)]\text{-}[(({}^{nP,Me}ArO)_3tacn)U^{IV}(N\text{-}CPh_3)]$ (**5a**) were obtained by slow benzene evaporation and were studied by XRD analysis.

The molecular structure of **5** in block-shaped crystals of **5a** shows one molecule of benzene coordinated to the potassium cation (Figure 2), which can be removed in high vacuum (as confirmed by CHN elemental analysis). Hence, all further characterizations were carried out with the benzene-free complex **5**. Again, the core structure of this imido complex is very similar to that of the penta- and hexavalent analogues. The most noticeable structural difference is the coordinated potassium ion that is weakly bound to the imido nitrogen (d_{K-N} = 2.943(2) Å), one aryloxide oxygen (d_{K-O} = 2.681(2) Å), one molecule of benzene ($d_{K-centroid}$ = 3.218 Å), and one aromatic ring of the trityl group ($d_{K\text{-}centroid}$ = 2.890 Å). The reduction to U^{IV}, however, influences the structural parameters within the U−NR group significantly, leading to an elongation of the $U-N_{imido}$ bond with a slightly longer $U-N_{imido}$ bond at

dx.doi.org/10.1021/ic5023517 | *Inorg. Chem.* 2014, 53, 13142−13153

2.036(2) Å and a shorter $N_{imido}-C_{trityl}$ bond distance of 1.455(3) Å. Nevertheless, the $U-N_{imido}$ bond still has significant multiple bond character, as $U^{IV}-N_{amido}$ bond lengths are typically much longer at ∼2.3 Å.[5l,25] The U≡NR triple bond is further confirmed by DFT studies (vide infra).

In accordance with the reduction from U^{V} in **3** to U^{IV} in **5**, the average $U-O_{ArO}$ and $U-N_{tacn}$ bond distances are longer, namely, 2.280 and 2.794 Å. Notably, the $U-O_{ArO}$ bond involved in the bonding interaction with the K ion is significantly longer (2.339(2) Å) than any other $U-O_{ArO}$ bond distances reported for related uranium complexes of the $(^{R,R'}ArO)_3tacn^{3-}$ ligand (2.15−2.26 Å).[5d,e,7,16] The $U-N_{imido}-C_{trityl}$ angle of 153.3(2)° is significantly more bent than the analogous $U-N_{imido}-C_{trityl}$ angles in **3** (165°) and **4** (179°), respectively, which is likely also a caused by the coordinated potassium ion.[2,21,24b]

Similar observations were made by Cummins et al. for the U^{V} trimethylsilyl imido complex with d_{U-N} = 1.943(4) Å and ∠($U-N_{imido}-Si$) = 170.25° and its analogous $Li{\cdot}U^{IV}$ trimethylsilyl imido complex with d_{U-NLi} = 2.050(3) Å and ∠($U-N_{imido}-Si$) = 150.35°.[5f]

The metric parameters of all complexes of the $[((^{nP,Me}ArO)_3tacn)U\text{-}(N\text{-}CPh_3)]^{-/0/+}$ series also compare well with the recently published U^{V} and U^{IV} tritylimido complexes $[((SiMe_3)_2N)_3U(N\text{-}CPh_3)]^{0/-}$. The molecular structure of the U^{IV} tritylimido anion $[((SiMe_3)_2N)_3U^{IV}(N\text{-}CPh_3)]^{-}$ also exhibits a coordinated potassium ion but is only coordinated to the trityl unit and not to the nitrogen atom of the imido ligand as described herein. In the latter, the U−N bond distance is reported at 1.993(2) Å with an angle ∠($U-N_{imido}-C$) of 169.8(2)°.[1b]

Complex **5** shows a paramagnetically shifted ^{1}H NMR spectrum (see Supporting Information, Figure S4) in a range from 110 to −125 ppm with relatively broad signals typical for U^{IV} tacn complexes. Although the molecular structure in the solid state is C_1 symmetrical, the ^{1}H NMR spectrum of **5** in solution exhibits C_3 symmetry with 11 detectable signals (15 signals are expected, of which four are likely paramagnetically shifted and broadened beyond detection). Each diastereotopic hydrogen atom gives rise to signals with very similar shifts leading to broad singlet signals. Accordingly, full assignment of all signals is hampered, but signal integration unambiguously identifies the methyl and *t*-butyl groups with singlet signals at −6.10 and −14.76 ppm, respectively, confirming the C_3 symmetry in solution

Stirring a hot toluene solution of **3** (120 °C) for 2 d yields the amido complex **6** $[((^{nP,Me}ArO)_3tacn)U^{IV}(N(H)\text{-}CPh_3)]$. Alternatively, amido species **6** can be synthesized from the U^{III} starting complex **1** by reaction with tritylamine (see Supporting Information). After stirring and filtration, complex **6** is obtained as an off-white solid in moderate yields. Single, pale green crystals of **6** were isolated from a concentrated THF solution at −35 °C. The molecular structure determined is almost identical to those of imido complexes **3**, **4**, and **5**, but with a H atom bound to the trityl nitrogen atom. This leads to the smallest of all $U-N-C_{trityl}$ angles (148.2(2)°) observed in this series of complexes. While the average $U-O_{ArO}$ and $U-N_{tacn}$ bond distances of 2.209 and 2.699 Å, respectively, do not differ much from those of complexes **3**−**5**, the $U-N_{amido}$ bond distance is significantly elongated and determined to be 2.253(3) Å. This value is comparable to other uranium amido bond lengths reported in literature and is consistent with a U═N double bond (see DFT analysis as well, vide infra).

Similar to imido **5**, amido species **6** exhibits paramagnetically shifted but relatively sharp resonances in the ^{1}H NMR spectrum, ranging from 95 to −115 ppm (see Supporting Information, Figure S5). On the basis of the C_3 symmetry in solution, 15 peaks are expected for the C−H signals and can be observed accordingly. Likely due to broadening, the N−H resonance is beyond detection, as also reported by Hayton et al. for $[Li(12\text{-crown-}4)_2][((SiMe_3)_2N)_3U(N(H)\text{-}CPh_3)]$.[25a] In contrast to the signals in the ^{1}H NMR spectrum of **5**, those of **6** are very sharp, well-separated, and thus can be integrated and assigned without difficulty. The methyl and *t*-butyl groups give rise to singlet resonances at −5.24 and −7.40 ppm, respectively. The H atoms of the aromatic rings of the trityl ligand appear as three signals in a 6:6:3 ratio, and the two more intense ones at δ = 35.89 and 9.33 ppm can be assigned to the trityl's ortho and meta hydrogen atoms. All other signals can be integrated to three protons each, corresponding to the remaining diastereotopic Hs of the chelating, tacn-anchored tris(aryloxide) ligand (see Supporting Information, Figure S5).

■ ELECTRONIC STRUCTURES AND MAGNETISM

The electronic absorption spectra of complexes **3**−**6** were recorded in the UV−vis and near-infrared (NIR) regions (Figure 3; for more details on complexes **2** and **7**, see Supporting Information, Figures S11 and S13). The black U^{VI} complex **4** absorbs strongly over the entire range of the spectrum from the UV to the NIR (see Supporting Information, Figure S10), with one strong absorption band centered at 278 nm (ε = 21 × 10^3 M^{-1} cm^{-1}) and multiple shoulders at approximately 400, 550, and 900 nm with molar

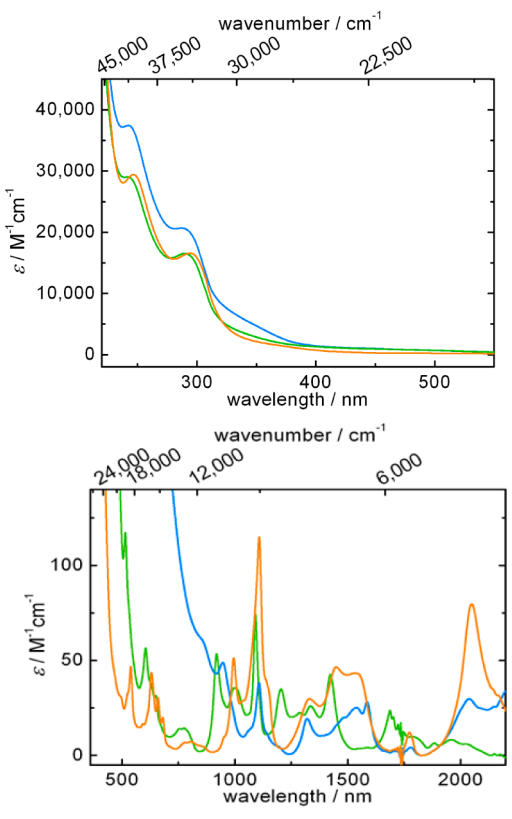

Figure 3. (top) UV−vis absorption spectra of **3** (blue), **5** (green), and **6** (orange). (bottom) Visible−NIR absorption spectra of **3** (blue), **5** (green), and **6** (orange).

dx.doi.org/10.1021/ic5023517 | Inorg. Chem. 2014, 53, 13142−13153

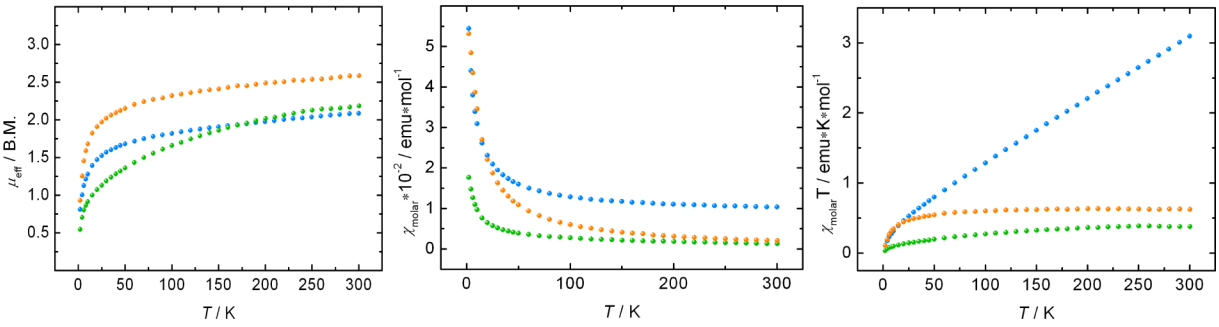

Figure 4. Temperature-dependent magnetic susceptibility data for **3** (blue), **5** (green), and **6** (orange), shown as plots of μ_{eff} vs T (left), χ vs T (middle), and χT vs T (right).

extinction coefficients of 7130, 4140, and 790 M^{-1} cm^{-1}, respectively. Above 1200 nm no absorption bands are observed due to the lack of f-electrons and their corresponding f−f transitions. Similarly, in the spectra of the pale green U^{IV} (**5**) and (**6**) and brown U^{V} (**3**) complexes, the UV−vis region from 200 to 700 nm is dominated by two intense and broad charge transfer (CT) $\pi \rightarrow \pi^*$ and $\pi \rightarrow nb_{5f}$ (nb = nonbonding) absorption bands with two distinct features at ∼250 nm (ε = 25−37 × 10^3 M^{-1} cm^{-1}) and ∼300 nm (ε = 15−20 × 10^3 M^{-1} cm^{-1}). Above 350 nm, however, the U^{V} (**3**) and U^{IV} complexes (**5**) and (**6**) show a number of sharp, low-intensity absorption bands between 500 and 2300 nm with ε = 10−115 M^{-1} cm^{-1}, typically arising from metal-centered f−f transitions in complexes with $5f^1$ and $5f^2$ valence electronic configurations.

An interesting spectral difference between the U^{IV} and U^{V} complexes is the bathochromic shift of the CT when going from the tetravalent amido complex **6** (480 nm) to imido **5** (520 nm). This shift is even more pronounced when going from the U^{IV} imido **5** to the U^{V} imido complex **3** (750 nm). The energetically more facile red shift of the charge-transfer transitions is expected with increasing covalency when going from U^{IV} amido (**6**) to U^{IV} imido (**5**) and even more so with increasing oxidation state, when going from U^{IV} imido (**5**) to U^{V} imido (**3**).

Variable-temperature superconducting quantum interference device (VT SQUID) magnetization data (2−300 K) were measured for complexes **3**, **5**, and **6** (complex **4** is diamagnetic) (Figure 4 and Table 2). For more details on complexes **2** and **7**, see Supporting Information, Figures S31−33.

Table 2. Magnetic Moments of the Complexes at 300 and 2 K

	μ_{eff} at 2 K [B.M.]	μ_{eff} at 300 K [B.M.]
3	0.81	2.09
5	0.54	2.18
6	0.93	2.59

One must be cautious when making general statements relating the different behavior in direct-current magnetic data with the degree of metal−ligand covalency. The origin of the different temperature dependency of the magnetic moment could be due to a change in the ligand-field splitting. The latter, however, is affected by the strength of the ligand, cf. covalency. Accordingly, a DFT computational analysis was conducted to quantify the degree of covalency in the series of complexes presented here (vide infra). This study supports the proposed relationship between the magnetic behavior and the degree of covalency within the uranium imido and amido moieties.

Complex **3** shows typical U^{V} behavior with a linear χT versus T above 25 K and strong temperature-dependency at 300 K, which indicates that only the first excited state is occupied and no further states become thermally populated over this temperature range. Overall, the magnetic moments (2 K: 0.81 μ_B, 300 K: 2.09 μ_B) are comparable to those reported for the mesitylimido complex [((^{nP,Me}ArO)$_3$tacn)U^{V}(N-mes)$_{eq}$], with a magnetic moment of 1.89 μ_B at 300 K and a slightly higher value at 2 K (1.22 μ_B).[15] The latter complex derivative has the imido ligand coordinated in an *equatorial* position, which leads to a significantly different crystal field. Regardless, the structurally similar mesitylimido complexes [(($^{R,t\text{-}Bu}$ArO)$_3$tacn)-U^{V}(N-mes)$_{ax}$], with the imido ligand coordinated in the *axial* position, possess significantly higher room temperature moments of 2.35 μ_B (R = *t*-Bu) and 2.40 μ_B (R = Ad) than those of **3**. Consequently, tritylimido complex **3** appears to have a stronger, more covalent uranium−nitrogen bond as compared to the other imido complexes of this ligand class. This assessment is in accordance with the observed U−NR bond distances of the other complex derivatives (^{nP,Me}U−N$_{trityl}$: 1.939(3) Å, $^{t\text{-}Bu,t\text{-}Bu}$U−N$_{mesityl}$: 2.047(8) Å, $^{Ad,t\text{-}Bu}$U−N$_{TMS}$: 2.122(2) Å).[5d,e] This is also in line with the general observation that the magnetic moment of a pentavalent uranium complex with a strongly bound π-donor ligand is considerably lower than that of the U^{V} free-ion moment of 2.54 μ_B ($^2F_{5/2}$).[26] The covalent interactions of the π-donor ligand decrease the magnetic moment by reducing the orbital angular momentum of the complex.[5g,27] Influenced by the structural and electronic differences within the U−N(H/K)-CPh$_3$ unit, tetravalent complexes [((^{nP,Me}ArO)$_3$tacn)U^{IV}(N(**K**)-CPh$_3$)] (**5**) and [((^{nP,Me}ArO)$_3$tacn)U^{IV}(N(**H**)-CPh$_3$)] (**6**) show markedly different magnetization curves. The U^{IV} ions in **5** and **6** possess a $^3H_4$ ground term and, as expected, the μ_{eff} values deviate significantly from the value for the free ion at 300 K (3.58 μ_B). Both U^{IV} complexes, imido **5** and amido **6**, do not show temperature-independent paramagnetism (TIP) but - in agreement with the two different axially bound ligands - do exhibit distinctly different temperature dependencies. The magnetic moment of imido complex **5** (μ_{eff} = 0.54 μ_B at 2 K) is increasing continuously with increasing temperature, which is characteristic of the ions non-magnetic ground state, and exhibits a rather low magnetic moment of 2.18 μ_B at 300 K. Amido complex **6**, on the other hand, shows a very different magnetic behavior with a relatively high low-temperature moment of μ_{eff} = 0.93 μ_B at 2 K that rapidly increases to 1.96 μ_B at 25 K. Above 60 K, the magnetic moment is almost

dx.doi.org/10.1021/ic5023517 | Inorg. Chem. 2014, 53, 13142−13153

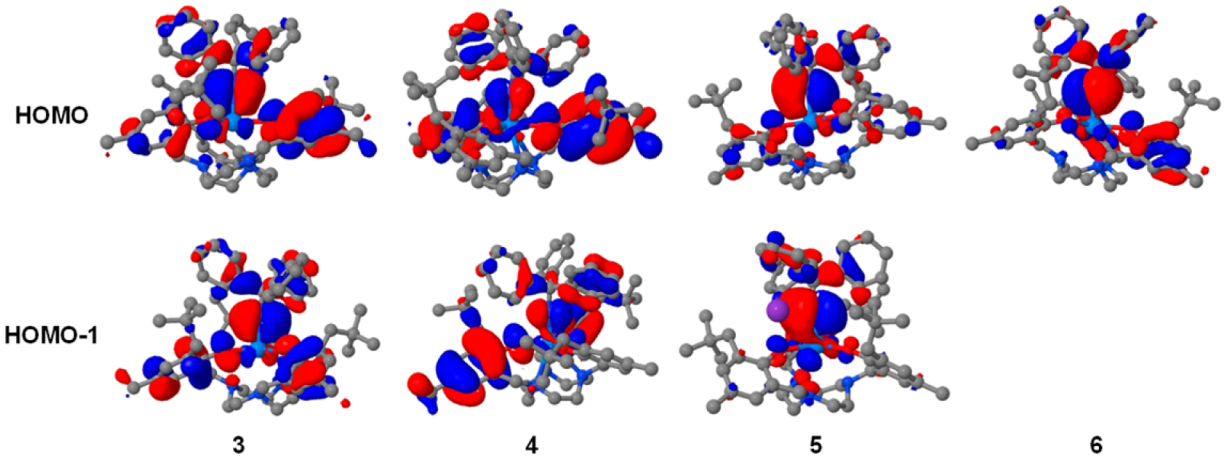

Figure 5. Bonding π-orbitals for the U^{V} imido complex **3**, the U^{VI} imido complex **4**, the U^{IV} imido complex **5**, and the U^{IV} amido complex **6**.

constant at ~2.3 μ_B with a room temperature moment of 2.59 μ_B at 300 K, which is significantly higher than the one observed in **5**. One reason for these differences may be the varying participation of the f-electrons in the U−N bonds of both U^{IV} complexes. Additionally, the possible overlap of the free p-orbitals of the nitrogen atom with the uranium f-electrons will influence the magnetic moment of the uranium ion. Thus, the different magnetism reflects the degree of covalency within the U−L bond in these two complexes. The bonding order is higher for complex **5** with the more covalently, formally triple-bonded axial imido ligand compared to the double-bonded amido ligand in **6**. Accordingly, imido **5** has a lower magnetic moment at room temperature. Remarkably, this is despite the chemical and structural similarity of **5** and **6**. This conclusion is further supported by DFT analysis, the different U−N bond distances ($U-N_{imido}$: 2.036(2) Å, $U-N_{amido}$: 2.253(3) Å), as well as the different bathochromic shifts of the CT (λ_{imido}: 520 nm, λ_{amido}: 480 nm).[5c,28]

DFT CALCULATIONS

To get insights into the bonding situation and the influence of the uranium oxidation state on the U−N multiple bond, DFT calculations (B3PW91/U (RECP)/6-31G** all other atoms) were carried out. Full geometry optimization was conducted without any symmetry constraints or any simplification of the supporting ligands. For all systems, the molecular orbitals (MOs) were carefully scrutinized. For the three imido complexes **3**, **4**, and **5**, two π-bonding orbitals were identified, whereas only one was found for the amido complex **6** (Figure 5).

This is the most obvious difference to lanthanide amido complexes that do not have reported π-interactions.[29] The presence of π-bonding orbitals is therefore diagnostic for the generally considered more covalent bonding picture in uranium complexes. The π-bonding orbitals are found to be an overlap of a uranium hybrid f/d-orbital with a pure p-orbital of the amido/imido nitrogen. To quantify the importance of the 5f-orbitals in bonding, f-in-core calculations were carried out. In all four cases, the Wiberg indices[30] were determined to estimate the influence of the oxidation state (if any) on the covalency.

In case of the amido **6**, a U−N bond index of 0.47 is in line with a fairly polarized (ionic) bond. In contrast, the imido complex **5** of U^{IV} is found to be significantly more covalent with a bond index of 0.88 (roughly twice of that compared to the amido). Moving from U^{IV} to U^{V} leads to an increase of the bond index to 1.24 and, consequently, to an increase of covalency. Finally, the most covalently bound imido is found in the U^{VI} species, possessing a Wiberg index of 1.58. Accordingly, with an increase of oxidation states in $[((^{nP,Me}ArO)_3tacn)U(N\text{-}CPh_3)]^{-/0/+}$, the tritylimido ligand is stronger bound and more covalent. Having in mind that the reactivity of uranium imido complexes **3**−**5** with CO_2 (vide infra) is based on multiple bond metathesis reactions, requiring a strongly polarized transition state, the least covalent U^{IV} amido complex **6** was expected to be the most reactive, and the U^{VI} imido complex **4** was expected to be the least reactive species. This is in excellent agreement with the CO_2 reactivity study reported herein (vide infra). Qualitatively, the DFT computational analysis also confirms the complexes' electronic structure description. The increasing covalency in complexes **6**, **5**, **3**, and **4** is well-documented by the red-shifted charge transfer bands as well as the overall low room-temperature magnetic moments, as observed in the complexes' UV−vis and SQUID magnetization studies (except for diamagnetic **4**).

REACTIVITY WITH CO_2

To probe the reactivity of the U−N multiple bond as a function of formal oxidation state, imido complexes **3**, **4**, and **5** as well as amido **6** were treated with carbon dioxide. The CO_2 reactant was chosen as a test substrate and for convenient comparison to the reported reactivity of closely related compounds of the tacn-based tris(aryloxide) chelate system.

For instance, the U^{IV} amido species **6** inserts CO_2 with formation of the carbamate $[((^{nP,Me}ArO)_3tacn)U^{IV}(\kappa^2\text{-}O_2C\text{-}N(H)CPh_3)]$ (**7**), a reaction that has previously been studied in detail (for full characterization, including molecular structure, see Supporting Information).[5e]

In contrast, imido complexes of the tris(aryloxide) ligand system generally react in a multiple-bond metathesis to yield the corresponding oxo complexes. For instance, U^{V} imido species **3** reacts with CO_2 under loss of tritylisocyanate (confirmed by IR analysis with $\nu_{N=C=O}$ = 2253 cm^{-1}, see Supporting Information, Figure S22) to the known U^{V} bis-μ-oxo complex $[\{((^{nP,Me}ArO)_3tacn)U^{V}\}_2(\mu\text{-}O)_2]$ (**9**).[15] The CO_2-mediated transformation of an imido to an oxo complex has also been reported for other U^{V} imido complexes[5e,m,15,22] and, thus, appears to be quite characteristic for U^{V} imido complexes of the tris(aryloxide) tacn-based chelate.

The observed reactivity of tritylimido complex **3**, however, is somewhat surprising, considering the sterically exceptionally

dx.doi.org/10.1021/ic5023517 | Inorg. Chem. 2014, 53, 13142−13153

demanding trityl group. This steric bulk does not appear to block access of the CO_2 to the U≡N bond, thus allowing for multiple-bond metathesis. This demonstrates the ability of the tris(aryloxide) tacn system to act as a stabilizing but flexible ligand, permitting further reactivity of the U−NR functional group. In agreement with the DFT calculations, hexavalent complex **4** does not show any reactivity with CO_2, but the tetravalent imido complex **5** reacts by changing color to pale green upon CO_2 exposure of the complex in THF solution. While IR analyses of the reaction mixture unambiguously confirm the formation of trityl isocyanate ($\nu_{N=C=O}$ = 2253 cm^{-1}) all efforts to crystallize this uranium complex **8** were unsuccessful. The formation of the known dinuclear U^{IV}/U^{IV} bis-μ-oxo complex, analogous to that obtained from the reaction of U^V complex **3** with CO_2 and subsequent reduction, can be excluded by ^{1}H NMR and IR studies. Additionally, ^{1}H NMR studies prove the absence of Gomberg's dimer that forms after elimination of a trityl radical. Initial evidence for the formation of a terminal oxo species comes from elemental analysis data that match for one calculated molecule of $K[((^{nP,Me}ArO)_3tacn)U^{IV}(O)]$ **8** and one molecule of trityl isocyanate; however, separation of the isocyanate byproduct remained unsuccessful. On the basis of all data available, we are confident in proposing the formation of a terminal, mononuclear U^{IV} oxo complex $K[((^{nP,Me}ArO)_3tacn)U^{IV}(O)]$ (**8**). A similar reaction to a terminal U^{IV} oxo complex via a multiple-bond metathesis reaction was reported by Bart and co-workers, where a U^{IV} imido was treated with *p*-tolualdehyde, resulting in the terminal U^{IV} oxo complex $[Tp^*_2U(O)]$ (Tp^* = hydrotris(3,5-dimethylpyrazolyl)borate) along with formation of the free imine.[5m]

CONCLUSION

The comprehensive reactivity study of the trivalent uranium precursor $[((^{nP,Me}ArO)_3tacn)U^{III}]$ (**1**) with the organic azides Me_3SiN_3, Me_3SnN_3, and Ph_3CN_3 is reported. While the reaction with Me_3SiN_3 yields an inseparable mixture of both the azido and imido uranium complexes, applying the heavier Sn homologue yields the bis-μ-azido complex $[\{((^{nP,Me}ArO)_3tacn)U^{IV}\}_2(\mu\text{-}\kappa^1\text{:}\kappa^1\text{-}N_3)_2]$ (**2**) exclusively. Surprisingly, only the reaction of **1** with tritylazide leads to two-electron oxidization and the desired U^V imido $[((^{nP,Me}ArO)_3tacn)U^V(N\text{-}CPh_3)]$ (**3**). Chemical oxidation and reduction of the U^V imido species **3** yield the corresponding U^{VI} and U^{IV} complexes $[((^{nP,Me}ArO)_3tacn)U^{VI}(N\text{-}CPh_3)][B(C_6F_5)_4]$ (**4**) and $K[((^{nP,Me}ArO)_3tacn)U^{IV}(N\text{-}CPh_3)]$ (**5**), respectively. In addition, an H atom abstraction reaction of U^V imido **3** with toluene provided access to the related U^{IV} amido complex $[((^{nP,Me}ArO)_3tacn)U^{IV}(N(H)CPh_3)]$ (**6**), which is intimately related to imido complex **5**. The tritylimido complexes **3**, **4**, and **5**, as well as amido complex **6**, were fully characterized by single-crystal XRD studies, CHN elemental analyses, ^{1}H NMR, IR vibrational, and UV−vis−NIR absorption spectroscopy as well as SQUID magnetization. Complexes **3** and **5** were also synthesized from ^{15}N-labeled tritylazide and characterized by IR and Raman vibrational spectroscopy. The structural continuity across the series of complexes in different oxidation states opened a unique opportunity to study the electronic properties. Accordingly, a DFT computational analysis complemented this study and provided evidence for U−N bond covalency and f-orbital participation in complexes **3**−**6**. With largely unperturbed complex core structures and a gradual change in covalency, this series additionally provided an opportunity to probe the uranium imido reactivity as a function of the nature of the U−N bond and the imido complexes' electron count. Thus, the CO_2 reactivity of the series of U^{IV}−U^{VI} complexes with largely unperturbed core structures was probed. The results show that the U^{VI} imido complex does not react with CO_2, while the U^V and U^{IV} imido species engage in multiple-bond metathesis reactions, yielding the corresponding uranium oxo species with concomitant formation of the isocyanate. In contrast, amido complex **6** inserts CO_2 in its U−N bond, forming the carbamate species **7**. Summarizing all CO_2 reactivity studies, we conclude that the covalent U≡N multiple bond in uranium imido complexes **3**, **4**, and **5** preferentially undergoes multiple-bond metathesis, while the amido complex **6**, with its more ionic U═N double bond, reacts with CO_2 in an insertion reaction. These findings agree well with the computational analysis of the U−N bond within this series of complexes. Future studies will help to generalize these findings on uranium imido reactivity and open new avenues to small-molecule activation by redox-active uranium complexes.

EXPERIMENTAL SECTION

General Considerations. All air- and moisture-sensitive experiments were performed under dry dinitrogen atmosphere, using standard Schlenk techniques or an MBraun inert-gas glovebox that has an atmosphere of purified dinitrogen and is equipped with a −35 °C freezer. Solvents were purified using a two-column, solid-state purification system (GlassContour System, Irvine, CA), transferred to the glovebox without exposure to air, and stored over molecular sieves and sodium (where appropriate). NMR solvents were obtained packaged under argon and stored over activated molecular sieves and sodium (where appropriate) prior to use. Carbon dioxide (99.8%, used as received) was purchased from Aldrich. ^{15}N-labeled sodium azide (enrichment: 98 atom % ^{15}N, used as received) was purchased from Cambridge Isotope Laboratories. Potassium intercalated graphite KC_8 and tritylazide were synthesized according to literature procedure.[31] ^{1}H NMR spectra were recorded on a JEOL ECX 400 MHz instrument at a probe temperature of 23 °C. Chemical shifts, δ, are reported relative to residual ^{1}H resonances of the solvent in ppm.[32] For convenience, and because of the intricacy of the complexes' NMR spectra, the full ^{1}H NMR spectra are shown in the Supporting Information. Electronic absorption spectra were recorded from 250 to 2200 nm (Shimadzu, UV-3600) in THF at room temperature. IR vibrational spectra were recorded from 3500 to 400 cm^{-1} (Shimadzu, IRAffinity-1) as KBr pellets at room temperature. Raman vibrational spectra were recorded on solids with an excitation wavelength of 1064 nm and a liquid N_2-cooled germanium detector (FT-Raman spectrometer RFS100 from Bruker) at room temperature. Magnetization data of microcrystalline and powdered samples (15−30 mg) were recorded with a SQUID magnetometer (Quantum Design) at different fields (0.1−5 T) and varying temperatures (2−300 K). Values of the magnetic susceptibility were corrected for the underlying diamagnetic increment by using tabulated Pascal constants and the effect of the blank sample holders (gelatin capsule/straw). Samples used for magnetization measurement were recrystallized and checked for chemical composition and purity by elemental analysis (C, H, and N) and ^{1}H NMR spectroscopy. Data reproducibility was carefully checked on three independently synthesized and measured samples. Elemental analyses were obtained using Euro EA 3000 (Euro Vector) and EA 1108 (Carlo-Erba) elemental analyzers in the Chair of Inorganic and General Chemistry at Friedrich-Alexander University Erlangen−Nürnberg (FAU) (except for fluoride-containing complex **3**, where the possible formation of hazardous, volatile UF_6 precluded elemental analysis).

Computational Details. All quantum-chemical calculations were conducted using the Gaussian09 program suite.[33] As functional, the Becke's three-parameter hybrid was applied, combined with the

dx.doi.org/10.1021/ic5023517 | Inorg. Chem. 2014, 53, 13142−13153

nonlocal correlation functional provided by Perdew–Wang, denoted as B3PW91.[34] Two different effective core potentials from Stuttgart–Dresden were used for describing the uranium atoms. The relativistic energy-consistent small-core pseudopotential of the Stuttgart–Köln ECP library was used in combination with its adapted segmented basis.[35] For comparison, the corresponding 5f-in-core ECP augmented by an f polarization function was used.[36] Note that this computational scheme was also applied previously by our group in analogous studies.[37] For all other atoms, a standard 6-31G** basis set was used.[38] All stationary points were identified as minima (number of imaginary frequencies Nimag = 0) or transition states (Nimag = 1).

Synthesis of [{((^{nP,Me}ArO)$_3$tacn)U^{IV}}$_2$(μ-N$_3$)$_2$] (2). A 20 mL scintillation vial was charged with [((^{nP,Me}ArO)$_3$tacn)U^{III}] (**1**) (0.200 g, 0.214 mmol) in 10 mL of THF. To this stirred dark red solution trimethyl stannane azide (0.044 g, 0.214 mmol), dissolved in 2 mL of THF, was added dropwise, resulting in an immediate color change to pale green. The solvent was removed in vacuo, and the remaining powder was dissolved in 5 mL of *n*-pentane to yield a pale green precipitate. The precipitate was removed by filtration and dried in vacuo to yield 156.5 mg (0.081 mmol, 75%) of **2** as a pale green solid. Green crystals suitable for XRD were obtained by slow evaporation of a benzene solution of **2**. ^{1}H NMR (400 MHz, C_6D_6): δ = 109.96, 52.33, 50.55, 44.46, 37.08, 23.68, 15.70, −0.05, −4.37, −5.65, −5.92, −6.50, −7.53, −7.97, −8.27, −19.70, −21.84, −32.25, −38.22, −127.82 ppm. Anal. Calcd [$C_{90}H_{132}N_{12}O_6U_2$, M = 1954.15 g/mol]: (calculated) C 55.32%, H 6.81%, N 8.60%; (found) C 55.23%, H 6.99%, N 7.76%. IR (KBr): ν = 3391, 2949 ν_{as}(CH$_2$), ν_s(CH$_3$), 2904 ν(CH$_2$), 2862 ν_s(CH$_2$), 2060 ν_{as}(N$_3$), 1607 ν(C═C), 1469 δ(CH$_2$), δ_{as}(CH$_3$), 1387, 1360, 1342, 1304 δ_ω(CH$_2$), 1275 ν_s(CO), δ(O–C═O), 1250 ν(CO), 1163 ν(CN), 1101 ν(CO), 1065, 1004, 953, 889 δ_{oop}(CH$_{Ar}$), 864 δ_{oop}(CH$_{Ar}$), 818 δ_{oop}(CH$_{Ar}$), 781 δ(O–C═O), 725, 534 ν(C–C), 515 cm^{-1}.

Synthesis of [((^{nP,Me}ArO)$_3$tacn)U^{V}(N-CPh$_3$)] (3). A 20 mL scintillation vial was charged with [((^{nP,Me}ArO)$_3$tacn)U^{III}] (**1**) (1.00 g, 1.07 mmol) in 10 mL of diethyl ether. Tritylazide (0.31 g, 1.07 mmol) was dissolved in diethyl ether and added to the uranium solution under vigorous stirring. With concomitant evolution of N_2 gas, the color changed from dark red to green-brown. After 30 min, the solvent was removed in vacuo, and the remaining powder was dissolved in 10 mL of *n*-pentane to yield a brown precipitate. The precipitate was removed by filtration and dried in vacuo to give 0.81 g (0.68 mmol, 64%) of **3** as a brown solid. Dark brown crystals suitable for XRD were obtained by slow diffusion of *n*-pentane into a solution of **3** in benzene. ^{1}H NMR (400 MHz, C_6D_6): δ = 45.46, 24.96, 22.50, 16.48, 11.86, 9.85 (CPh$_3$), 8.81 (CPh$_3$), 7.85 (CPh$_3$), 6.87, 6.41, 5.87, 3.55, 1.87 (CPh$_3$), 1.41, 1.05, 0.21, −0.53 (Me), −2.97 (^{t}Bu), −4.78 (^{t}Bu), −5.88, −7.12, −8.74, −9.56 ppm. Anal. Calcd [$C_{64}H_{81}N_4O_3U$, M = 1191.68 g/mol]: (calculated) C 64.47%, H 6.85%, N 4.70%; (found) C 63.92%, H 6.89%, N 4.67%. IR (KBr): ν = 3056 (CPh$_3$), 2947 ν_{as}(CH$_2$), ν_s(CH$_3$), 2904 ν(CH$_2$), 2862 ν_s(CH$_2$), ν_{as}(CH$_3$), 1605 ν(C═C), 1466 δ(CH$_2$), δ_{as}(CH$_3$), 1443, 1362, 1309 δ_ω(CH$_2$), 1254 ν(CO), 1165 ν(CN), 1104 ν(CO), 1064, 1030, 1003, 957, 887 δ_{oop}(CH$_{Ar}$), 864 δ_{oop}(CH$_{Ar}$), 818 δ_{oop}(CH$_{Ar}$), 779, 760 (CPh$_3$), 698 (CPh$_3$), 632 (CPh$_3$), 517 cm^{-1}.

Synthesis of [((^{nP,Me}ArO)$_3$tacn)U^{VI}(N-CPh$_3$)][B(C$_6$F$_5$)$_3$] (4). A 20 mL scintillation vial was charged with [((^{nP,Me}ArO)$_3$tacn)U^{V}(N-CPh$_3$)] (**3**) (0.497 g, 0.042 mmol) in 3 mL of benzene. AgBAr$_{F20}$ was added to the stirred green solution, which led to an immediate color change to black. After 1 h, the solvent was removed in vacuo, and the remaining powder was dissolved in 3 mL of *n*-pentane to form a black precipitate, which was removed by filtration and dried in vacuo to yield 36.2 mg (0.019 mmol, 47%) of **4** as a black solid. Black crystals suitable for XRD were obtained by slow evaporation of a benzene solution of **4**. ^{1}H NMR (400 MHz, THF-d_8): δ = 7.61 (Ar), 7.52 (Ar), 7.22 (CPh$_3$), 6.98 (CPh$_3$), 5.14, 3.67, 3.49 (Me), 3.36, 3.22, 3.17, 2.99, 2.19, 1.00 (*t*-Bu) ppm. IR (KBr): ν = 3056 (CPh$_3$), 2947 ν_{as}(CH$_2$), ν_s(CH$_3$), 2904 ν(CH$_2$), 2862 ν_s(CH$_2$), ν_{as}(CH$_3$), 1605 ν(C═C), 1643 (BAr$_{F20}$), 1512 (BAr$_{F20}$), 1466 δ(CH$_2$), δ_{as}(CH$_3$), 1443, 1362, 1309 δ_ω(CH$_2$), 1254 ν(CO), 1223 (BAr$_{F20}$), 1188 (BAr$_{F20}$), 1165 ν(CN), 1104 ν(CO), 1092 (BAr$_{F20}$), 1064, 1030, 1003, 980 (BAr$_{F20}$), 957, 887 δ_{oop}(CH$_{Ar}$), 864 δ_{oop}(CH$_{Ar}$), 818 δ_{oop}(CH$_{Ar}$), 779, 760 (CPh$_3$), 698 (CPh$_3$), 660 (BAr$_{F20}$), 632 (CPh$_3$), 517 cm^{-1}.

Synthesis of K[((^{nP,Me}ArO)$_3$tacn)U^{IV}(N-CPh$_3$)] (5). A 20 mL scintillation vial was charged with [((^{nP,Me}ArO)$_3$tacn)U^{V}(N-CPh$_3$)] (**3**) (0.300 g, 0.252 mmol) in 10 mL of benzene. KC_8 (0.041 mg, 0.302 mmol) was added to the nonstirring dark red solution. After 6 h, during which time the suspension was occasionally shaken, the entire KC_8 turned black, and the solution turned yellow-green. The solid was filtered through a Celite pad, and the solvent was removed in vacuo. The remaining powder was dissolved in 5 mL of *n*-pentane to yield a yellow-green precipitate, which was vigorously stirred. The precipitate was removed by filtration and dried in vacuo to yield 0.239 mg (0.191 mmol, 76%) of **5** as a yellow-green solid. Yellow-green crystals suitable for XRD were obtained by slow evaporation of a benzene solution of **5**. ^{1}H NMR (400 MHz, C_6D_6): δ = 108.50, 52.22 (CPh$_3$), 43.93 (CPh$_3$), 12.10, 10.98, 3.22, −6.10 (Me), −8.02, −14.76 (^{t}Bu), −27.82, −123.19 ppm. Anal. Calcd [$C_{64}H_{81}KN_4O_3U$, M = 1231.48 g/mol]: (calculated) C 62.42%, H 6.63%, N 4.55%; (found) C 62.03%, H 6.67%, N 4.75%. IR (KBr): ν = 3056 (CPh$_3$), 2947 ν_{as}(CH$_2$), ν_s(CH$_3$), 2904 ν(CH$_2$), 2862 ν_s(CH$_2$), ν_{as}(CH$_3$), 2831, 1605 ν(C═C), 1466 δ(CH$_2$), δ_{as}(CH$_3$), 1443, 1362, 1309 δ_ω(CH$_2$), 1254 ν(CO), 1165 ν(CN), 1104 ν(CO), 1096, 1064, 1030, 1003, 957, 887 δ_{oop}(CH$_{Ar}$), 864 δ_{oop}(CH$_{Ar}$), 806 δ_{oop}(CH$_{Ar}$), 779, 760 (CPh$_3$), 698 (CPh$_3$), 632 (CPh$_3$), 503 cm^{-1}.

Synthesis of [((^{nP,Me}ArO)$_3$tacn)U^{IV}(N(H)-CPh$_3$)] (6). From **1**: A J. Young NMR tube was charged with [((^{nP,Me}ArO)$_3$tacn)U^{III}] (**1**) (0.020 g, 0.021 mmol) dissolved in 1 mL of benzene-d_6, and tritylamine (0.005 mg, 0.021 mmol) was added leading to a slight color change. After 1 h, the reaction was checked by ^{1}H NMR spectroscopy, confirming complete reaction and formation of complex pure **6**.

From **3**: A J. Young NMR tube was charged with [((^{nP,Me}ArO)$_3$tacn)U^{V}(N-CPh$_3$)] (**3**) (0.020 g, 0.017 mmol) dissolved in 1 mL of toluene-d_6. The solution was heated to 120 °C and checked by ^{1}H NMR spectroscopy from time to time. After 2 d, the reaction was checked by ^{1}H NMR spectroscopy, confirming complete reaction and formation of complex **6**.

From **5**: A 20 mL scintillation vial was charged with K-[((^{nP,Me}ArO)$_3$tacn)U^{IV}(N-CPh$_3$)] (**5**) (0.100 g, 0.082 mmol), and 10 mL of acetonitrile was added. This led to an immediate precipitation of an off-white solid. After 30 min of vigorous stirring, the solid was removed by filtration and dried in vacuo to give 0.052 g (0.044 mmol, 54%) of pure **6** as an off-white solid. Pale green crystals suitable for X-ray diffraction were obtained from a concentrated THF solution at −35 °C. ^{1}H NMR (400 MHz, C_6D_6): δ = 94.72, 45.73, 44.34, 35.89 (CPh$_3$), 9.33 (CPh$_3$), 9.12, −3.33, −5.24 (Me), −5.84, −6.25, −7.40 (^{t}Bu), −10.47, −21.71, −24.09, −113.79 ppm. Anal. Calcd [$C_{64}H_{82}N_4O_3U$, M = 1193.39 g/mol]: (calculated) C 64.41%, H 6.93%, N 4.69%; (found) C 63.53%, H 6.82%, N 4.96%. IR (KBr): ν = 3056 (CPh$_3$), 2947 ν_{as}(CH$_2$), ν_s(CH$_3$), 2904 ν(CH$_2$), 2862 ν_s(CH$_2$), ν_{as}(CH$_3$), 1605 ν(C═C), 1466 δ(CH$_2$), δ_{as}(CH$_3$), 1443, 1362, 1309 δ_ω(CH$_2$), 1254 ν(CO), 1165 ν(CN), 1104 ν(CO), 1049, 1030, 1003, 957, 887 δ_{oop}(CH$_{Ar}$), 864 δ_{oop}(CH$_{Ar}$), 818 δ_{oop}(CH$_{Ar}$), 779, 760 (CPh$_3$), 698 (CPh$_3$), 632 (CPh$_3$), 517 cm^{-1}.

Synthesis of [((^{nP,Me}ArO)$_3$tacn)U^{IV}(κ^2-O$_2$C–N(H)-CPh$_3$)] (7). A 20 mL scintillation vial was charged with [((^{nP,Me}ArO)$_3$tacn)U^{IV}(NH–CPh$_3$)] (**6**) (0.063 g, 0.053 mmol) in 10 mL of THF. Under vigorous stirring, CO_2 was introduced to the pale green solution over 15 min resulting in a colorless solution. The solvent was removed in vacuo, the remaining powder was dissolved in 1 mL of *n*-pentane to yield a pale green precipitate. The precipitate was removed by filtration and dried in vacuo to give 54.8 mg (0.044 mmol, 84%) of **7** as a pale green solid. ^{1}H NMR (400 MHz, C_6D_6): δ = 47.96, 36.35, 33.40, 29.55, 25.00, 18.68, 14.99, 9.28, 6.73, 6.23, 0.08, −2.88, −7.90, −13.47, −29.95, −33.50, −39.62, −43.96, −53.13, −71.05 ppm. Anal. Calcd [$C_{65}H_{82}N_4O_5U$, M = 1237.40 g/mol]: (calculated) C 63.09%, H 6.68%, N 4.53%; (found) C 63.47%, H 6.61%, N 4.49%. IR (KBr): ν = 3449 (NH), 3059 (CPh$_3$), 2947 ν_{as}(CH$_2$), ν_s(CH$_3$), 2904 ν(CH$_2$), 2862 ν_s(CH$_2$), ν_{as}(CH$_3$), 1605 ν(C═C), 1558 (C–N), 1492 (C═O), 1469 δ(CH$_2$), δ_{as}(CH$_3$), 1443, 1362, 1307 δ_ω(CH$_2$), 1254 ν(CO),

dx.doi.org/10.1021/ic5023517 | Inorg. Chem. 2014, 53, 13142–13153

1165 ν(CN), 1104 ν(CO), 1049, 1030, 957, 891 $\delta_{oop}(CH_{Ar})$, 860 $\delta_{oop}(CH_{Ar})$, 818 $\delta_{oop}(CH_{Ar})$, 783, 760 (CPh_3), 725, 702 (CPh_3), 663, 624 (CPh_3), 532, 509 cm^{-1}.

Synthesis of K[((^{nP,Me}ArO)$_3$tacn)U^{IV}(O)] (8). A 20 mL scintillation vial was charged with K[((^{nP,Me}ArO)$_3$tacn)U^{IV}(N-CPh_3)] (**5**) (0.010 g, 0.008 mmol) in 2 mL of THF. Under stirring, CO_2 was introduced to the yellow-green solution over 2 h, resulting in a color change to bright green. The solvent was removed in vacuo, and the solids were dissolved in 1 mL of *n*-pentane to yield a green precipitate, which was removed by filtration and dried in vacuo. IR spectroscopy shows a band at 2253 cm^{-1}, corresponding to the C−N stretch of tritylisocyanate. Additionally, the elemental analysis fits for the terminal U^{IV} oxo complex **8** with 1 equiv of trityl isocyanate. Multiple attempts to crystallize and/or separate complex **8** from the isocyanate remained unsuccessful. ^{1}H NMR (400 MHz, THF-d_8): δ = 46.92, 35.79, 33.11, 28.28, 26.01, 18.38, 13.88, 10.74, 8.94, 7.34, 6.89, 6.73, 6.57, 4.70, 1.78, 0.92, −3.16, −3.88, −9.17, −13.86, −30.39 ppm. Anal. Calcd [($C_{45}H_{66}N_3O_4U$)K_2($C_{20}H_{15}NO$), M = 1275.49 g/mol]: (calculated) C 61.21%, H 6.40%, N 4.39%; (found) C 59.80%, H 6.46%, N 4.61%. IR (KBr): ν = 2947 $\nu_{as}(CH_2)$, $\nu_s(CH_3)$, 2904 $\nu(CH_2)$, 2862 $\nu_s(CH_2)$, $\nu_{as}(CH_3)$, 2253 (C−N), 2075, 1605 ν(C═C), 1578 (C−N), 1543, 1466 (C═O), $\delta(CH_2)$, $\delta_{as}(CH_3)$, 1443, 1362, 1307 $\delta_{\omega}(CH_2)$, 1254 ν(CO), 1165 ν(CN), 1104 ν(CO), 1072, 1034, 957, 891 $\delta_{oop}(CH_{Ar})$, 860 $\delta_{oop}(CH_{Ar})$, 818 $\delta_{oop}(CH_{Ar})$, 783, 760 (CPh_3), 729, 702 (CPh_3), 629 (CPh_3), 509 cm^{-1}.

Synthesis of [{((^{nP,Me}ArO)$_3$tacn)U^{V}}$_2$(μ-O)$_2$] (9). A J. Young NMR tube was charged with [((^{nP,Me}ArO)$_3$tacn)U^{V}(N-CPh_3)] (**3**) (0.020 g, 0.017 mmol) dissolved in 1 mL of benzene-d_6. CO_2 was added to the solution without color change. After 1 h, the reaction was checked by ^{1}H NMR and IR spectroscopy, confirming the formation of complex **9** and tritylisocyanate. ^{1}H NMR (400 MHz, C_6D_6): δ = 9.58, 8.97, 8.85, 7.64, 6.72, 5.27, 4.29 (3H, Me), 3.88, 3.47, 3.26 (Me), 1.37 (^{t}Bu), 0.09 (^{t}Bu), −2.30, −3.21, −3.52 ppm. IR (KBr): 2253 (C−N) cm^{-1} for the resulting tritylisocyanate.

■ ASSOCIATED CONTENT

Ⓢ Supporting Information

Supporting graphics, experimental conditions, synthetic procedures, and spectroscopic data. This material is available free of charge via the Internet at http://pubs.acs.org.

■ AUTHOR INFORMATION

Corresponding Author

*E-mail: karsten.meyer@fau.de.

Notes

The authors declare no competing financial interest.

■ ACKNOWLEDGMENTS

The Bundesministerium für Bildung und Forschung (BMBF 2020+, Support Codes 02NUK012C and 02NUK010C), the FAU Erlangen-Nürnberg, and COST Action CM1006.

■ REFERENCES

(1) (a) Hayton, T. W. *Dalton Trans.* **2010**, *39*, 1145. (b) Mullane, K. C.; Lewis, A. J.; Yin, H.; Carroll, P. J.; Schelter, E. J. *Inorg. Chem.* **2014**, *53*, 9129.

(2) (a) Pilyugina, T. S.; Schrock, R. R.; Hock, A. S.; Müller, P. *Organometallics* **2005**, *24*, 1929. (b) Ren, W.; Zi, G.; Walter, M. D. *Organometallics* **2012**, *31*, 672. (c) Franceschi, F.; Solari, E.; Floriani, C.; Rosi, M.; Chiesi-Villa, A.; Rizzoli, C. *Chem.—Eur. J.* **1999**, *5*, 708.

(3) In addition to the terminal uranium nitrides reported by Liddle et al., a number of complexes featuring bridging nitrido ligands have been reported in recent years, like Evans, W. J.; Kozimor, S. A.; Ziller, J. W. *Science* **2005**, *309*, 1835. Nocton, G.; Pécaut, J.; Mazzanti, M. *Angew. Chem., Int. Ed.* **2008**, *47*, 3040. Fox, A. R.; Arnold, P. L.; Cummins, C. C. *J. Am. Chem. Soc.* **2010**, *132*, 3250. Fortier, S.; Wu, G.; Hayton, T. W. *J. Am. Chem. Soc.* **2010**, *132*, 6888. Fox, A. R.; Cummins, C. C. *J. Am. Chem. Soc.* **2009**, *131*, 5716. Camp, C.; Pécaut, J.; Mazzanti, M. *J. Am. Chem. Soc.* **2013**, *135*, 12101.

(4) (a) King, D. M.; Tuna, F.; McInnes, E. J. L.; McMaster, J.; Lewis, W.; Blake, A. J.; Liddle, S. T. *Nat. Chem.* **2013**, *5*, 482. (b) King, D. M.; Tuna, F.; McInnes, E. J. L.; McMaster, J.; Lewis, W.; Blake, A. J.; Liddle, S. T. *Science* **2012**, *337*, 717.

(5) (a) Morris, D. E.; Da Re, R. E.; Jantunen, K. C.; Castro-Rodriguez, I.; Kiplinger, J. L. *Organometallics* **2004**, *23*, 5142. (b) Graves, C. R.; Yang, P.; Kozimor, S. A.; Vaughn, A. E.; Clark, D. L.; Conradson, S. D.; Schelter, E. J.; Scott, B. L.; Thompson, J. D.; Hay, P. J.; Morris, D. E.; Kiplinger, J. L. *J. Am. Chem. Soc.* **2008**, *130*, 5272. (c) Castro-Rodriguez, I.; Olsen, K.; Gantzel, P.; Meyer, K. *J. Am. Chem. Soc.* **2003**, *125*, 4565. (d) Castro-Rodriguez, I.; Nakai, H.; Meyer, K. *Angew. Chem., Int. Ed.* **2006**, *45*, 2389. (e) Bart, S. C.; Anthon, C.; Heinemann, F. W.; Bill, E.; Edelstein, N. M.; Meyer, K. *J. Am. Chem. Soc.* **2008**, *130*, 12536. (f) Vlaisavljevich, B.; Diaconescu, P. L.; Lukens, W. L.; Gagliardi, L.; Cummins, C. C. *Organometallics* **2013**, *32*, 1341. (g) Lam, O. P.; Franke, S. M.; Nakai, H.; Heinemann, F. W.; Hieringer, W.; Meyer, K. *Inorg. Chem.* **2012**, *51*, 6190. (h) Cladis, D. P.; Kiernicki, J. J.; Fanwick, P. E.; Bart, S. C. *Chem. Commun.* **2013**, *49*, 4169. (i) Zalkin, A.; Beshouri, S. M. *Acta Crystallogr. C* **1988**, *44*, 1826. (j) Brennan, J. G.; Andersen, R. A. *J. Am. Chem. Soc.* **1985**, *107*, 514. (k) Evans, W. J.; Traina, C. A.; Ziller, J. W. *J. Am. Chem. Soc.* **2009**, *131*, 17473. (l) Arney, D. S. J.; Burns, C. J. *J. Am. Chem. Soc.* **1995**, *117*, 9448. (m) Matson, E. M.; Crestani, M. G.; Fanwick, P. E.; Bart, S. C. *Dalton Trans.* **2012**, *41*, 7952. (n) Jilek, R. E.; Tomson, N. C.; Shook, R. L.; Scott, B. L.; Boncella, J. M. *Inorg. Chem.* **2014**, *53*, 9818. (o) Fortier, S.; Wu, G.; Hayton, T. W. *Dalton Trans.* **2010**, *39*, 352. (p) Burns, C. J.; Smith, W. H.; Huffman, J. C.; Sattelberger, A. P. *J. Am. Chem. Soc.* **1990**, *112*, 3237.

(6) Anderson, N. H.; Odoh, S. O.; Yao, Y.; Williams, U. J.; Schaefer, B. A.; Kiernicki, J. J.; Lewis, A. J.; Goshert, M. D.; Fanwick, P. E.; Schelter, E. J.; Walensky, J. R.; Gagliardi, L.; Bart, S. C. *Nat. Chem.* **2014**, *6*, 919.

(7) Schmidt, A.-C.; Nizovtsev, A. V.; Scheurer, A.; Heinemann, F. W.; Meyer, K. *Chem. Commun.* **2012**, *48*, 8634.

(8) Adeosun, S. O. *Inorg. Nucl. Chem. Letters* **1976**, *12*, 301.

(9) Gondzik, S.; Schulz, S.; Blaser, D.; Wolper, C.; Haack, R.; Jansen, G. *Chem. Commun.* **2014**, *50*, 927.

(10) (a) Prasad, L.; Gabe, E. J.; Glavincevski, B.; Brownstein, S. *Acta Crystallogr., Sect. C* **1983**, *39*, 181. (b) Bénaud, O.; Berthet, J.-C.; Thuéry, P.; Ephritikhine, M. *Inorg. Chem.* **2011**, *50*, 12204. (c) Thomson, R. K.; Cantat, T.; Scott, B. L.; Morris, D. E.; Batista, E. R.; Kiplinger, J. L. *Nat. Chem.* **2010**, *2*, 723.

(11) Crawford, M.-J.; Ellern, A.; Mayer, P. *Angew. Chem., Int. Ed.* **2005**, *44*, 7874.

(12) (a) Castro-Rodriguez, I.; Meyer, K. *J. Am. Chem. Soc.* **2005**, *127*, 11242. (b) Charpin, P.; Lance, M.; Nierlich, M.; Vigner, D.; Livet, J.; Musikas, C. *Acta Crystallogr., Sect. C* **1986**, *42*, 1691. (c) Berthet, J.-C.; Lance, M.; Nierlich, M.; Vigner, J.; Ephritikhine, M. *J. Organomet. Chem.* **1991**, *420*, C9. (d) Nocton, G.; Pécaut, J.; Mazzanti, M. *Angew. Chem., Int. Ed.* **2008**, *47*, 3040. (e) Evans, W. J.; Kozimor, S. A.; Ziller, J. W. *Science* **2005**, *309*, 1835.

(13) Evans, W. J.; Miller, K. A.; Ziller, J. W.; Greaves, J. *Inorg. Chem.* **2007**, *46*, 8008.

(14) (a) Turner, Z. R.; Bellabarba, R.; Tooze, R. P.; Arnold, P. L. *J. Am. Chem. Soc.* **2010**, *132*, 4050. (b) Arnold, P. L.; Liddle, S. T. *Chem. Commun.* **2005**, 5638.

(15) Schmidt, A.-C.; Heinemann, F. W.; Lukens, W. W.; Meyer, K. *J. Am. Chem. Soc.* **2014**, *136*, 11980.

(16) (a) Castro-Rodriguez, I.; Meyer, K. *Chem. Commun.* **2006**, 1353. (b) Lam, O. P.; Heinemann, F. W.; Meyer, K. *C. R. Chim.* **2010**, *13*, 803. (c) Kosog, B.; La Pierre, H. S.; Heinemann, F. W.; Liddle, S. T.; Meyer, K. *J. Am. Chem. Soc.* **2012**, *134*, 5284.

(17) Klapötke, T. M.; Nöth, H.; Schwenk-Kircher, H.; Walther, W.-H.; Holl, G. *Polyhedron* **1999**, *18*, 717.

(18) IR vibrational spectroscopy (see ESI) for complex **2** reveals the very strong asymmetric stretching vibration for the coordinated azide ligands at 2060 cm^{-1}, similar to one observed in [{(($^{t\text{-Bu},t\text{-Bu}}$ArO)$_3$tacn)

$U^{IV}\}_2(\mu\text{-}N_3)$] ($\nu_{as}(N_3^-)$ = 2074 cm^{-1})], see Castro-Rodriguez, I.; Meyer, K. *J. Am. Chem. Soc.* **2005**, *127*, 11242−11243.
(19) Goerlich, J. R.; Farkens, M.; Fischer, A.; Jones, P. G.; Schmutzler, R. *Z. Anorg. Allg. Chem.* **1994**, *620*, 707.
(20) Complex **3** is highly soluble and thus reduces the isolated yield.
(21) (a) Fenske, D.; Kujanek, R.; Dehnicke, K. *Z. Anorg. Allg. Chem.* **1983**, *507*, 51. (b) Abram, U.; Voigt, A.; Kirmse, R. *Polyhedron* **2000**, *19*, 1741. (c) Sellmann, D.; Wemple, M. W.; Donaubauer, W.; Heinemann, F. W. *Inorg. Chem.* **1997**, *36*, 1397.
(22) Hayton, T. W.; Boncella, J. M.; Scott, B. L.; Batista, E. R. *J. Am. Chem. Soc.* **2006**, *128*, 12622.
(23) Zalkin, A.; Brennan, J. G.; Andersen, R. A. *Acta Crystallogr., Sect. C* **1988**, *44*, 1553.
(24) (a) Bendix, J.; Anthon, C.; Schau-Magnussen, M.; Brock-Nannestad, T.; Vibenholt, J.; Rehman, M.; Sauer, S. P. A. *Angew. Chem., Int. Ed.* **2011**, *50*, 4480. (b) Scepaniak, J. J.; Young, J. A.; Bontchev, R. P.; Smith, J. M. *Angew. Chem., Int. Ed.* **2009**, *48*, 3158.
(25) (a) Smiles, D. E.; Wu, G.; Hayton, T. W. *J. Am. Chem. Soc.* **2013**, *136*, 96. (b) Stewart, J. L.; Andersen, R. A. *Polyhedron* **1998**, *17*, 953.
(26) Kindra, D. R.; Evans, W. J. *Chem. Rev.* **2014**, *114*, 8865.
(27) (a) Fortier, S.; Brown, J. L.; Kaltsoyannis, N.; Wu, G.; Hayton, T. W. *Inorg. Chem.* **2012**, *51*, 1625. (b) Lukens, W. W.; Edelstein, N. M.; Magnani, N.; Hayton, T. W.; Fortier, S.; Seaman, L. A. *J. Am. Chem. Soc.* **2013**, *135*, 10742. (c) Camp, C.; Antunes, M. A.; Garcia, G.; Ciofini, I.; Santos, I. C.; Pecaut, J.; Almeida, M.; Marcalo, J.; Mazzanti, M. *Chem. Sci.* **2014**, *5*, 841. (d) Arnold, P. L.; Jones, G. M.; Odoh, S. O.; Schreckenbach, G.; Magnani, N.; Love, J. B. *Nat. Chem.* **2012**, *4*, 221. (e) King, D. M.; Tuna, F.; McMaster, J.; Lewis, W.; Blake, A. J.; McInnes, E. J. L.; Liddle, S. T. *Angew. Chem., Int. Ed.* **2013**, *52*, 4921. (f) Lewis, A. J.; Nakamaru-Ogiso, E.; Kikkawa, J. M.; Carroll, P. J.; Schelter, E. J. *Chem. Commun.* **2012**, *48*, 4977.
(28) (a) Seaman, L. A.; Wu, G.; Edelstein, N.; Lukens, W. W.; Magnani, N.; Hayton, T. W. *J. Am. Chem. Soc.* **2012**, *134*, 4931. (b) Bart, S. C.; Heinemann, F. W.; Anthon, C.; Hauser, C.; Meyer, K. *Inorg. Chem.* **2009**, *48*, 9419. (c) Lam, O. P.; Feng, P. L.; Heinemann, F. W.; O'Connor, J. M.; Meyer, K. *J. Am. Chem. Soc.* **2008**, *130*, 2806.
(29) (a) Perrin, L.; Maron, L.; Eisenstein, O.; Lappert, M. F. *New J. Chem.* **2003**, *27*, 121. (b) Perrin, L.; Maron, L.; Eisenstein, O. *Faraday Discuss.* **2003**, *124*, 25.
(30) We have preferred discussing the Wiberg bond indexes over either Mulliken population or decomposition analysis. This is because (i) the Mulliken population is basis set dependent and (ii) the bonding in actinide complexes in general is not fully covalent. Accordingly, NBO or decomposition analyses are less appropriate techniques for the complexes discussed here.
(31) (a) Viculis, L. M.; Mack, J. J.; Mayer, O. M.; Hahn, H. T.; Kaner, R. B. *J. Mater. Chem.* **2005**, *15*, 974. (b) Saunders, W. H.; Ware, J. C. *J. Am. Chem. Soc.* **1958**, *80*, 3328.
(32) Fulmer, G. R.; Miller, A. J. M.; Sherden, N. H.; Gottlieb, H. E.; Nudelman, A.; Stoltz, B. M.; Bercaw, J. E.; Goldberg, K. I. *Organometallics* **2010**, *29*, 2176.
(33) Frisch, M. J.; Trucks, G. W.; Schlegel, H. B.; Scuseria, G. E.; Robb, M. A.; Cheeseman, J. R.; Scalmani, G.; Barone, V.; Mennucci, B.; Petersson, G. A.; Nakatsuji, H.; Caricato, M.; Li, X.; Hratchian, H. P.; Izmaylov, A. F.; Bloino, J.; Zheng, G.; Sonnenberg, J. L.; Hada, M.; Ehara, M.; Toyota, K.; Fukuda, R.; Hasegawa, J.; Ishida, M.; Nakajima, T.; Honda, Y.; Kitao, O.; Nakai, H.; Vreven, T.; Montgomery, J. A., Jr.; Peralta, J. E.; Ogliaro, F.; Bearpark, M.; Heyd, J. J.; Brothers, E.; Kudin, K. N.; Staroverov, V. N.; Kobayashi, R.; Normand, J.; Raghavachari, K.; Rendell, A.; Burant, J. C.; Iyengar, S. S.; Tomasi, J.; Cossi, M.; Rega, N.; Millam, J. M.; Klene, M.; Knox, J. E.; Cross, J. B.; Bakken, V.; Adamo, C.; Jaramillo, J.; Gomperts, R.; Stratmann, R. E.; Yazyev, O.; Austin, A. J.; Cammi, R.; Pomelli, C.; Ochterski, J. W.; Martin, R. L.; Morokuma, K.; Zakrzewski, V. G.; Voth, G. A.; Salvador, P.; Dannenberg, J. J.; Dapprich, S.; Daniels, A. D.; Farkas, O.; Foresman, J. B.; Ortiz, J. V.; Cioslowski, J.; Fox, D. J. *Gaussian 09*, Revision A.02; Gaussian, Inc.: Wallingford, CT, 2009.
(34) (a) Becke, A. D. *J. Chem. Phys.* **1993**, *98*, 5648. (b) Perdew, J. P.; Wang, Y. *Phys. Rev. B: Condens. Matter* **1992**, *45*, 13244.
(35) (a) Küchle, W.; Dolg, M.; Stoll, H.; Preuss, H. *J. Chem. Phys.* **1994**, *100*, 7535. (b) Cao, X.; Dolg, M.; Stoll, H. *J. Chem. Phys.* **2003**, *118*, 487. (c) Cao, X.; Dolg, M. *J. Mol. Struct.: THEOCHEM* **2004**, *673*, 203.
(36) (a) Moritz, A.; Cao, X.; Dolg, M. *Theor. Chem. Acc.* **2007**, *118*, 845. (b) Moritz, A.; Dolg, M. *Theor. Chem. Acc.* **2008**, *121*, 297.
(37) (a) Castro, L.; Yahia, A.; Maron, L. *Dalton Trans.* **2010**, *39*, 6682. (b) Castro, L.; Yahia, A.; Maron, L. *ChemPhysChem* **2010**, *11*, 990. (c) Kosog, B.; Kefalidis, C. E.; Heinemann, F. W.; Maron, L.; Meyer, K. *J. Am. Chem. Soc.* **2012**, *134*, 12792. (d) Mougel, V.; Camp, C.; Pécaut, J.; Copéret, C.; Maron, L.; Kefalidis, C. E.; Mazzanti, M. *Angew. Chem., Int. Ed.* **2012**, *51*, 12280. (e) Cooper, O.; Camp, C.; Pécaut, J.; Kefalidis, C. E.; Maron, L.; Gambarelli, S.; Mazzanti, M. *J. Am. Chem. Soc.* **2014**, *136*, 6716.
(38) (a) Hehre, W. J.; Ditchfield, R.; Pople, J. A. *J. Chem. Phys.* **1972**, *56*, 2257. (b) Hariharan, P. C.; Pople, J. A. *Theor. Chim. Acta* **1973**, *28*, 213.